Curr Pain Headache Rep (2015) 19: 16
DOI 10.1007/s11916-015-0489-9

IMAGING (L MECHTLER, SECTION EDITOR)

Neuroimaging of Headaches Associated with Vascular Disorders

Sabareesh K. Natarajan · Maxim Mokin · Ashish Sonig · Elad I. Levy

Published online: 28 May 2015

Abstract Headaches from vascular causes need to be differentiated from primary headaches because a misdiagnosis may lead to dire consequences for the patient. Neuroimaging is critical in identifying patients with vascular headaches and identifying the nature of the pathologic disorder causing these headaches. In addition, the imaging findings guide the physician regarding the optimal treatment modality for these lesions. This review summarizes the nuances of differentiating patients with secondary headaches related to vascular disease and discusses pertinent neuroimaging studies.

Keywords Cervical dissection · Headache · Neuroimaging · Vascular disorders · Vascular malformations

This article is part of the Topical Collection on *Imaging*

S. K. Natarajan · M. Mokin · A. Sonig · E. I. Levy (✉)
Department of Neurosurgery, School of Medicine and Biomedical Sciences, University at Buffalo, State University of New York, 100 High Street, Suite B4, Buffalo, NY 14203, USA
e-mail: elevy@ubns.com

S. K. Natarajan · M. Mokin · A. Sonig · E. I. Levy
Department of Neurosurgery, Gates Vascular Institute/Kaleida Health, Buffalo, NY, USA

M. Mokin
Departments of Neurology and Neurosurgery, University of South Florida College of Medicine, Tampa, FL, USA

E. I. Levy
Department of Radiology, School of Medicine and Biomedical Sciences, University at Buffalo, State University of New York, Buffalo, NY, USA

E. I. Levy
Toshiba Stroke and Vascular Research Center, University at Buffalo, State University of New York, Buffalo, NY, USA

Abbreviations

AVF	Arteriovenous fistula
AVM	Arteriovenous malformation
CE	Contrast enhanced
CSF	Cerebrospinal fluid
CT	Computed tomographic
CTA	Computed tomographic angiography
CVT	Cerebral venous thrombosis
DSA	Digital subtraction angiography
ECA	External carotid artery
FLAIR	Fluid-attenuated inversion recovery
GRE	Gradient echo
ICA	Internal carotid artery
ICH	Intracranial hemorrhage
MR	Magnetic resonance
MRA	Magnetic resonance angiography
RCVS	Reversible cerebral vasoconstriction syndrome
SAH	Subarachnoid hemorrhage
SWI	Susceptibility-weighted imaging
TOF	Time-of-flight
VA	Vertebral artery

Introduction

Headaches are a common reason for visiting a neurologist, a primary care physician, or an emergency department. It is important to differentiate patients presenting with headaches potentially arising from a secondary cause, especially a vascular cause. The International Classification of Headache Disorders (ICHD) II [1] recognizes headaches related to vascular disorders as secondary headaches (Table 1). The diagnosis is definite only when the headache resolves or greatly improves within a specified time after its onset or after the acute phase of the disorder. When this is not the case or before the specified

Table 1 Vascular headaches according to the International Classification of Headache Disorders (ICHD)

1. Headache attributed to ischemic stroke or transient ischemic attack
2. Headache attributed to nontraumatic intracranial hemorrhage
3. Headache attributed to unruptured vascular malformation
4. Headache attributed to arteritis
5. Carotid or vertebral artery pain
6. Headache attributed to cerebral venous thrombosis
7. Headache attributed to other intracranial vascular disorder

For all vascular headaches, the diagnostic criteria include, whenever possible:

A. Headache with one (or more) of the stated characteristics (if any are known) and fulfilling criteria C and D

B. Major diagnostic criteria of the vascular disorder

C. The temporal relationship of the association with, and/or other evidence of causation by, the vascular disorder

D. Improvement or disappearance of headache within a defined period after its onset or after the vascular disorder has remitted or after its acute phase

Adapted from reference [1]

time has elapsed, the diagnosis is qualified by stating "probably attributed to vascular disorder." Recognizing that these are criteria that cannot be applied in all instances, especially when the headache does not resolve or greatly improves after 3 months, leads to a diagnosis of chronic post-vascular-disorder headache. Features that suggest a secondary headache [2] include the following:

- systemic symptoms (fever, weight loss, fatigue)
- secondary risk factors (human immunodeficiency virus, cancer, immunodeficiency)
- neurologic symptoms or signs (altered mental status, focal deficits)
- sudden onset (split-second, thunderclap)
- older age onset (new onset after age 50)
- previous history/positional/papilledema/precipitants

Headaches Associated with Cerebral Aneurysms

Cerebral aneurysms are present in 2 % of the population, and there are 30,000 aneurysmal ruptures per year in the USA [3•]. The clinical presentation of aneurysmal subarachnoid hemorrhage (SAH) is very distinct. Approximately 80 % of awake patients relate a history of having the worst headache of their life, and 20 % give a history of a sentinel headache [4]. Symptomatic unruptured intracranial aneurysms in patients presenting with sentinel thunderclap headaches (episodes of sudden, intense headache with peak intensity at onset and resolution within the following 72 h) should be treated in principle as sentinel headaches have been reported to precede SAH in 10 to 50 % of patients [5, 6]. Additional signs and symptoms may include nausea and/or vomiting, stiff neck, a brief loss of consciousness, or focal neurological deficits (including cranial nerve palsies).

The mortality rate of aneurysmal SAH is 26–32 %, and the prognosis is best in patients who present to a medical facility without any neurological deficits [7]. The chances of rerupture and deterioration of neurological status are very high in the initial 7–10 days; hence, the need for a high index of suspicion to diagnose this entity. A noncontrast head CT scan will aid in the diagnosis of most cases of SAH (Fig. 1) if performed soon after the onset of headache. The sensitivity of this study decreases with time as the hemoglobin is metabolized and diluted. The sensitivity is 100 % at 6 h but decreases to percentages in the low 90 s by 24 h and less than 75 % within 2–3 days [8]. There have been reports that computed tomographic angiography (CTA) or magnetic resonance angiography (MRA) along with a noncontrast CT scan is sufficiently sensitive to exclude the presence of a SAH and a lumbar puncture may not be necessary [8]. A lumbar puncture should be performed after vascular imaging that shows an aneurysm if the noncontrast CT scan is negative and the patient is symptomatic. A CT scan along with CTA remains the method of choice because the time frame for imaging is shorter, the detail with CTA is finer, and the availability is greater. Large-sized (>12 mm) and medium-sized (7–12 mm) aneurysms are detected by CTA nearly 100 % of the time [9]. The detection rate for small-sized (<7 mm) and even medium-sized aneurysms from the anterior circulation near the skull base is 75–98 % [9]. The development of CTA with matched mask bone elimination [10] or dual-energy CT angiography [11] has lowered the radiation dose of a CT angiogram with good sensitivity for

Fig. 1 Noncontrast CT scan of the head showing diffuse basal cistern SAH and enlarged bilateral temporal horns suggestive of hydrocephalus

detecting cerebral aneurysms. Therefore, patients with a high clinical suspicion for an aneurysm who have a negative CT angiogram should undergo conventional 3D rotational digital subtraction angiography (DSA) [12, 13].

Fluid-attenuated inversion recovery (FLAIR) sequences in MR imaging demonstrate SAH with high (near 100 %) sensitivity [14] (Fig. 2). The change in T2 induced by red blood cells and by blood serum protein is sufficient to prevent fluid suppression in a FLAIR image and thus picks up SAH in FLAIR imaging, even in cases missed with CT imaging [15]. It is important to pay special attention to T2-weighted MR images of the brain and cervical spine to identify T2 flow voids from abnormal dilated vessels. These would direct further imaging to delineate underlying vascular pathology. Three basic MRA techniques [16] are most commonly used in a clinical setting: time-of-flight (TOF), phase-contrast, and 3D contrast-enhanced (CE). Contrast administration is not required for TOF and phase-contrast MR angiography but intrinsic problems with these techniques may lead to degradation of image quality, especially for aneurysm detection. These artifacts are more pronounced in aneurysms that are less than 5 mm. 3D CE MRA can overcome many of the problems encountered with TOF and phase-contrast techniques. Small aneurysms are likely to be undetected even with CE MRA due to limited spatial resolution.

The gold standard for aneurysm detection is conventional cerebral angiography. We perform a four-vessel angiogram (bilateral ICA and vertebral artery [VA]) with 3D rotational angiography of the suspect vessel in these patients to exclude the presence of a cerebral aneurysm and perform a six-vessel (bilateral ICA, VA, and external carotid artery [ECA]) angiogram if the four-vessel study is negative to rule out an arteriovenous fistula (AVF) in patients with intracranial hemorrhage (ICH). If the first angiogram is negative in a patient with SAH, we repeat the angiogram in 5–7 days, as the hemorrhagic event can induce thrombosis of the aneurysm and make the aneurysm undetectable on the first angiogram [17].

In patients at high risk for treatment because of aneurysm location, comorbidities, or old age, the risk versus benefit should be considered carefully. Isolated oculomotor nerve palsies are classically associated with unruptured posterior circulation aneurysms [18]. A posterior communicating artery aneurysm may compress the third nerve in the ambient cistern and manifest as a mydriatic pupil with a third nerve palsy in contrast to the third nerve palsy in diabetic patients in which the pupil is usually spared [19]. Internal carotid artery aneurysms in the cavernous sinus can present with a cavernous sinus syndrome involving cranial nerve palsies in 61 %, retrobulbar pain in 23 %, and trigeminal pain in 10 % of cases. The mechanism of cranial nerve palsies may include rapid growth, wall stretching, and abrupt formation of a bleb in the aneurysm sac and these may indicate an imminent rupture. In a series of 40 patients presenting with cavernous sinus syndrome, most treated patients improved or remained stable after treatment, but none improved without treatment [20].

In patients with unruptured aneurysms whom we decide to manage conservatively, regular noninvasive angiographic follow-up with CT angiography or MR angiography annually for 2–5 years and then every 2–5 years thereafter, control of hypertension, and cessation of smoking may be beneficial [21]. Aneurysms that increase in size or change in morphology or are associated with symptom progression during follow-up should be considered for treatment if the risk-benefit ratio of treatment is favorable [22].

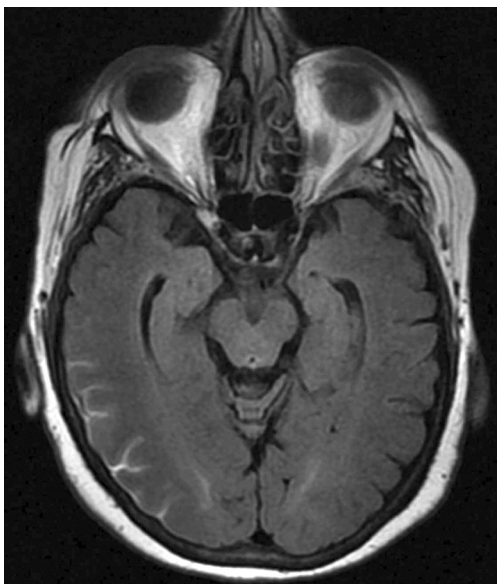

Fig. 2 FLAIR MR image showing convexity SAH in the right occipital region

Headaches Associated with Vascular Malformations

The three common vascular malformations associated with headache are arteriovenous malformations (AVMs), AVFs, and cavernomas.

AVMs

AVMs are arteriovenous shunts that consist of an abnormal capillary bed in the subpial space fed by arteries that normally feed the brain parenchyma and are drained by pial veins. Cortical AVMs involve the cortex, are fed exclusively by cortical arteries, and drain into superficial veins. These are always sulcal lesions and sometime referred to as pure pial AVMs. Cortical-subcortical AVMs are gyral AVMs that recruit cortical arteries and drain into the superficial venous system but may also drain into deep veins. Corticoventricular AVMs are the classic pyramidal lesions that are based in the cortex but reach the ventricles with the apex of the pyramid. These are

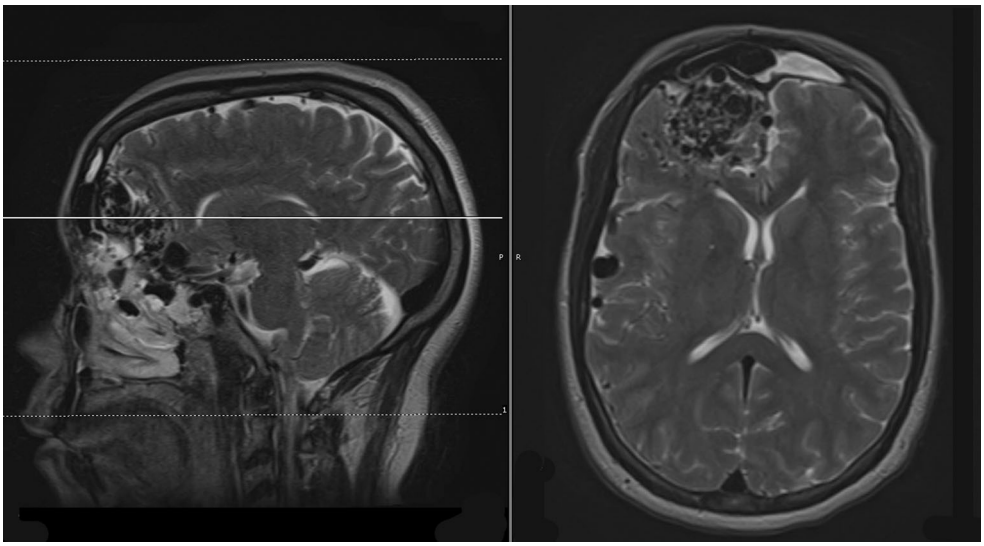

Fig. 3 Sagittal (*left*) and axial (*right*) T2 images of the brain showing a right frontal AVM with hypointense flow voids

fed by both cortical and deep perforating arteries and drain into both the superficial and deep venous system. Deep-seated AVMs involve the deep nuclei and recruit deep perforating arteries exclusively. The arterial and venous connections are along the long fiber tracts. Choroid plexus AVMs are important to recognize, as they are anatomically extracerebral and accessible to surgical treatment. They are fed by choroidal arteries and subependymal cortical feeders and drain via ventricular veins.

Contemporary series report less than 50 % of AVMs manifesting with headache and hemorrhage [23]. The average annual risk of rupture of a symptomatic unruptured AVM is estimated to be 2–4 and 33 % of AVMs manifest with headaches [24, 25]. Headaches are more commonly seen in children with AVMs. AVMs in occipital locations, those having transdural supply, venous ectasia, and venous congestion are more commonly associated with headaches. Venous congestion can be identified by T2 or FLAIR sequences showing brain edema in the venous territory. A conventional angiogram can delineate the transdural supply of the AVM from the ECA circulation or dilation of the venous outflow to form venous ectasias. Destabilization of the hemodynamics of an AVM causes hemorrhage. Features that increase the risk of future hemorrhage in an AVM are MR imaging evidence of previous hemorrhage, deep brain location, deep venous drainage, presence of an intranidal aneurysm, and restriction of venous drainage by stenosis or thrombosis [26, 27]. These features are important to identify, because these AVMs are more likely to be treated than observed after performing a thorough risk-benefit analysis in each patient. Small AVMs are difficult to see on noncontrast CT scans. Larger AVMs can be seen as hyperdense structures because of pooling of blood in the AVM or draining veins. A CE CT scan or CTA may show an abnormal tangle of vessels, feeding artery aneurysm, or enlarged draining veins. 4D time-resolved CTA that captures multiple volumes of the brain in the arterial venous phases can demonstrate early filling of venous structures in the arterial phase of imaging, thus confirming the presence of an AVM [28••]. T2-weighted MR images show punctate to linear flow voids in the parenchyma or subarachnoid space (Fig. 3). TOF and phase-contrast MR angiography may aid the detection of these lesions but do not detail the angioarchitecture. This is true only for 4D CE MRA. 3D contrast-enhanced MRA provides the velocity and direction of flow through the AVM and can help to confirm the diagnosis (Fig. 4). Dynamic MRA, similar to 4D CTA, separates arterial, capillary, and venous phases to identify and understand AVMs better than standard MRA. However, 4D MRA has lower spatial resolution than 3D CE MRA and is not ideal for evaluation of the microstructure.

Conventional six-vessel angiography is essential to confirm the presence of an AVM and to assess the angioarchitecture in detail. Increased flow in the arteries

Fig. 4 Coronal reconstruction of a dynamic CTA in the later arterial phase showing a right frontal AVM filling from the right middle cerebral artery branches with a draining vein to the superior sagittal sinus

supplying the AVM results in enlargement and tortuosity of those arteries and the development of feeding artery aneurysms in 10–15 % of cases. Half of the AVMs contain an enlarged vessel in the nidus denoting an intranidal aneurysm. Early opacification of the draining vein in the arterial phase is the hallmark of diagnosis of an AVM or fistula. Parametric imaging provides a novel approach to displaying an entire DSA imaging sequence (arterial, capillary, and venous phases of radiographic contrast filling) as a single composite image. Early experience with parametric imaging (Fig. 5) suggests that this technique is especially useful in evaluating AVMs with a complex flow pattern, such as those with multiple pedicles, to distinguish abnormal feeders from normal arteries and veins [29].

Arteriovenous Fistulas

Dural AVFs are abnormal connections between arteries that would normally supply the meninges, bone, and muscle and small venules in the walls of the venous sinuses, but not the brain. Adult-type dural AVFs are acquired lesions postulated to be formed after venous sinus thrombosis, recanalization, and development of AV shunts from neovascularization or enlargement of preexisting connections in the walls of the sinus [30]. One third to one half of dural AVFs are found at the transverse sigmoid junction. Cavernous fistulas are the second commonest and are classified as direct if they have a direct connection between the cavernous sinus and the ICA and indirect if they are fed by multiple ECA branches or dural branches of the ICA. Dural AVFs are considered aggressive or malignant when they show cortical or spinal reflux and are associated with an 8.1 % annual risk of ICH and an annual mortality of 10.4 % [31]. Direction of venous outflow drainage (antegrade vs retrograde) contributes to an understanding of grading and treatment options [32]. Higher grade lesions with cortical venous reflex have a higher propensity to present with headaches or hemorrhagic strokes. A CT scan may show hyperdense venous thrombosis and MR imaging may show multiple flow voids around the cavernous sinus or transverse-sigmoid sinus. 4D CTA or 3D CE MRA may confirm the presence of an AVF by identifying an early draining vein. In cases of carotid cavernous fistula, proptosis, enlargement of the superior ophthalmic vein, and edema of retroorbital fat may be seen [33]. Conventional six-vessel angiography is the gold standard for assessing the angioarchitecture and planning treatment for these lesions [32].

Cavernous Malformation

Cavernous malformations are compact masses of sinusoidal vessels without intervening brain parenchyma. They are angiographically occult and may have a developmental venous anomaly that is demonstrated by angiography. Familial cavernomatous malformations are common in Hispanic population and more often are multiple and transmitted by autosomal dominant mutations. Most of these lesions are not detectable by CT imaging. They may appear as hyperdense lesions with or without calcifications and acute hemorrhage. MR T2-weighted images, T2-weighted gradient echo (GRE) sequences (Figs. 6 and 7), and susceptibility-weighted imaging (SWI) sequences are the best sequences for detecting cavernomas. Cavernomas appear as popcorn lesions consisting of a reticulated heterogeneous core surrounded by a hypointense hemosiderin ring. GRE sequences demonstrate a prominent susceptibility effect (blooming), and SWI sequences show more smaller lesions than GRE sequences [34]. Acute hemorrhage can show surrounding edema on T2-weighted images. Cavernomas are classified as four types: I, hyperintense on both T1 and T2 sequences; II (classic), mixed hyperintense and hypointense core surrounded by a hypointense core on T2 sequences; III, hypointense on both T1 and T2 sequences; and IV, hypointense only on GRE and SWI sequences and these are usually asymptomatic [35]. MR tractography, especially of the corticospinal tract, may facilitate surgical removal of these lesions in periventricular or brainstem locations by allowing the surgeon to plan safe

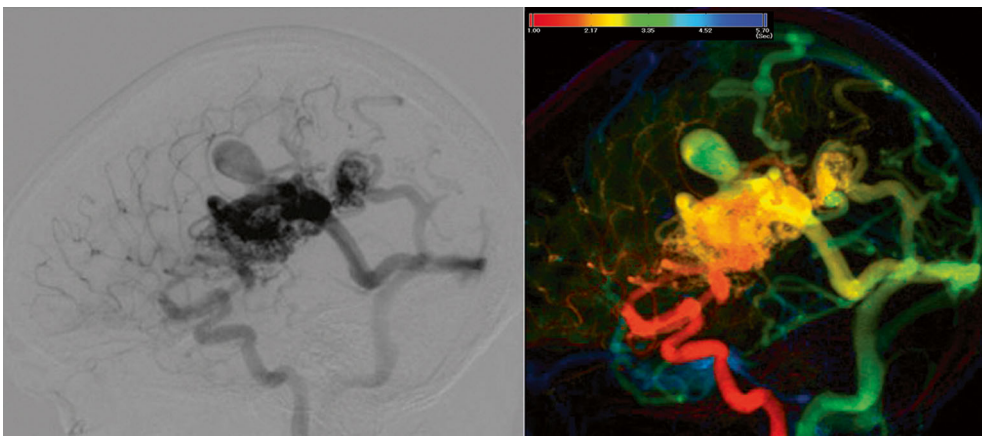

Fig. 5 Parametric reconstruction of a lateral view ICA injection angiogram. The imaging on the *left* shows a posterotemporal AVM. Parametric imaging of the same AVM (*right*) showing different times-to-peak of contrast material in different parts of the AVM coded by *different colors*

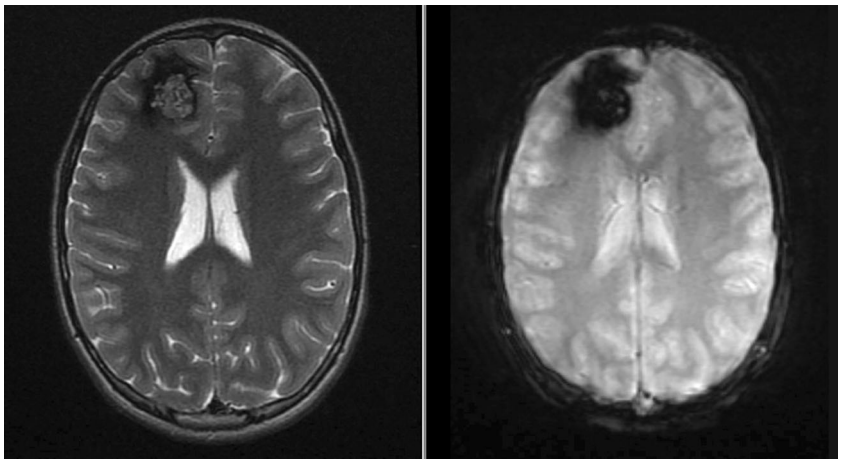

Fig. 6 T2 fast spin echo (FSE) axial (*left*) and T2 gradient echo (GRE) axial (*right*) images showing a right frontal cavernoma with a mulberry appearance on FSE imaging and blooming artifact due to the hemorrhage on GRE imaging

trajectories that avoid the corticospinal tract in order to approach these lesions.

The commonest cause of headaches in cavernomas is hemorrhage. Hemorrhage in cavernomas can be classified into intralesional or extralesional. Intralesional hemorrhage occurs inside the gliotic capsule of the cavernoma, enlarges the cavernoma by osmotic effect, and is less likely to cause neurological deficits. A weakened capsule with hemodynamic stress leads to extralesional hemorrhage and has a higher risk of causing neurological deficits and ICH. Extralesional hemorrhage can be differentiated by MR imaging that shows acute or subacute blood beyond the hemosiderin ring; cavernomas with extralesional blood may need to be treated more aggressively [36].

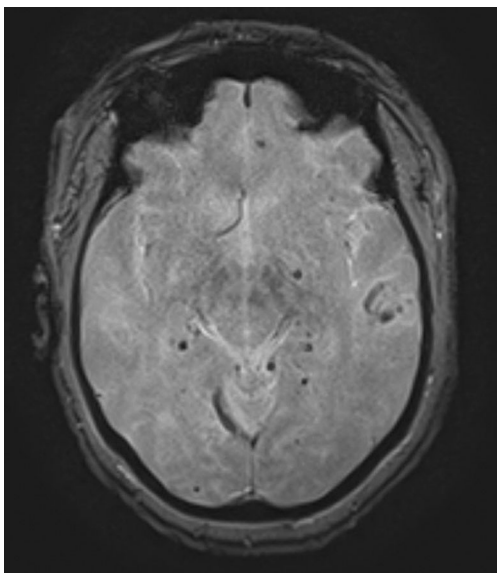

Fig. 7 GRE axial sequence showing multiple hypointensities consistent with blood degradation products. The commonest cause of multiple hyopintensities in GRE sequences is multiple cavernomas (rarely, amyloid angiopathy or chronic traumatic encephalopathy is responsible for such an imaging appearance)

Headache Associated with Cerebral Venous Thrombosis

Cerebral venous thrombosis (CVT) is a rare cause of stroke (accounting for 0.5 % of all strokes). Prothrombotic situations, such as oral contraceptive use, malignancy, dehydration, and inherited thrombophilia, predispose to CVT. The four clinical syndromes associated with CVT include (1) intracranial hypertension, (2) focal neurological strokes due to edema or hemorrhage, (3) encephalopathy (altered mental status or decreased level of consciousness), or (4) seizures [37]. Headache is the commonest symptom, affecting 90 % of patients with CVT [38, 39]. Although making a "clinical diagnosis" is difficult because of the indolent presentation, imaging diagnosis is easy in most cases, and rapid anticoagulation can be lifesaving in these patients. Imaging is performed to view the thrombus or the consequences of thrombus in the brain parenchyma or venous flow pattern. On CT imaging, acute thrombus can be seen as hyperdensity within venous sinuses in 20 % of cases [40••]. There may be indirect signs of CVT, such as brain edema, hemorrhage, or infarction, that may be detected by CT imaging although MR imaging may show these better. CE CT imaging may show a filling defect in the sinus (empty delta sign) surrounded by intense enhancement of the sinus wall (Fig. 8). CT venograms show 3D reconstructions of the venous system that facilitate detection and assess progression or resolution of CVT with treatment. On MR images, the presence of hyperintensity within the sinus on a GRE sequence in conjunction with hypointensity on the T2 sequence is indicative of venous patency. Absence of T2 flow void and hypointensity on GRE sequences is characteristic of CVT (Fig. 8) [40••]. CE MR imaging and MRA may be employed similar to CT venography for assessment of CVT. MR has the advantages of less exposure to radiation and utilizing a safer contrast agent and allows better assessment of indirect consequences of CVT. 4D CTA and dynamic MRA are useful in observing the changes in flow pattern that result as a consequence of CVT. Dynamic MR venography has shown a

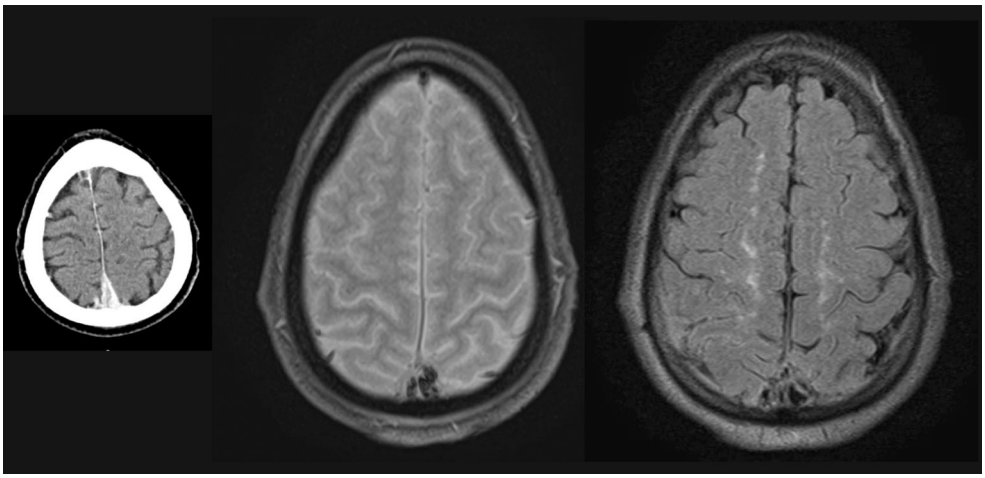

Fig. 8 *Left*, contrast axial CT image showing a filling defect in the superior sagittal sinus surrounded by intense contrast enhancement. *Center*, GRE axial image in the same patient showing hypointensity. *Right*, FLAIR axial imaging show corresponding absence of T2 flow voids

significantly higher sensitivity for detecting dural venous sinus thrombosis when compared to regular TOF MR venography [41]. Conventional angiography is currently performed only for treatment of CVT and not for diagnosis.

Headaches Due to Cervical Artery Dissection

Extracranial carotid artery and vertebral artery dissections, often referred to as cervical dissection, are an important cause of stroke in younger patients. The estimated annual incidence rates are 2–5 cases per 100,000 persons for carotid artery dissection and 1 case per 100,000 persons for vertebral artery dissection [42, 43]. Trauma is a frequent cause of cervical dissection, making a thorough history important in establishing the correct diagnosis. Although an association between cervical dissection and cervical manipulative therapy (chiropractor manipulation) has been established, on the basis of clinical reports and population-control studies, the 2014 American Heart Association/American Stroke Association scientific statement concluded there is insufficient evidence to establish the claim that mechanical forces generated during such manipulative therapy are the cause of the dissection [44].

Unilateral headache, neck, and jaw pain are the classic clinical findings, although bilateral distribution of symptoms from dissections involving bilateral carotid or vertebral arteries has been reported as well [45–47]. Horner's syndrome from irritation of the sympathetic fibers of the internal carotid plexus is suggestive of carotid artery dissection. Ischemic symptoms can be quite variable, depending on the brain

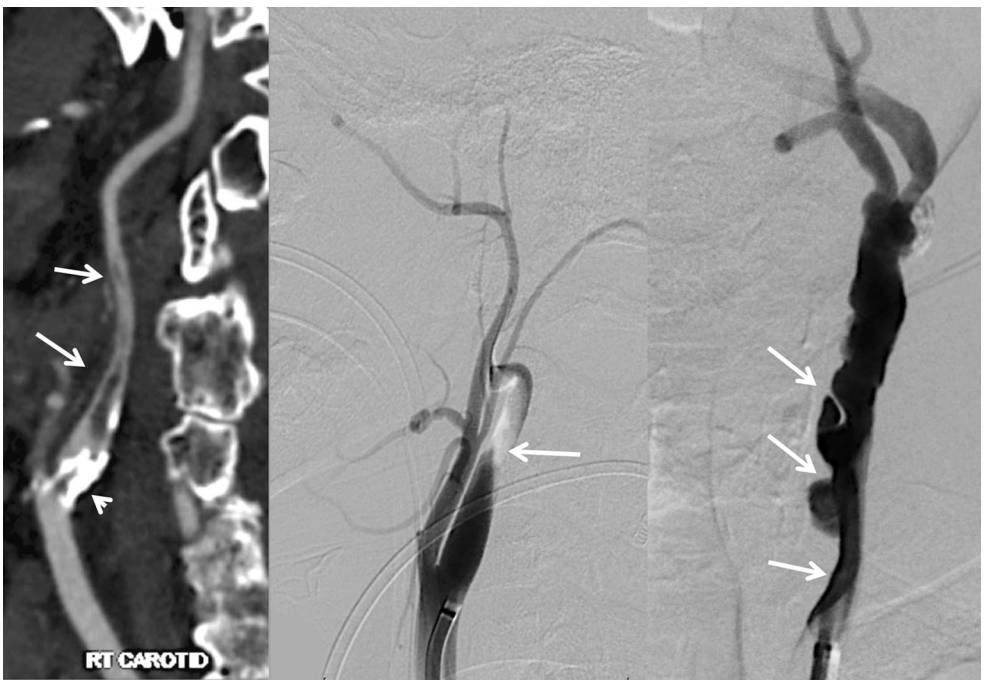

Fig. 9 Angiographic appearance of carotid artery dissection. *Left*, CT angiogram demonstrating a filling defect (*arrows*) at the origin of the ICA, cervical segment, secondary to a dissection flap. Hyperdense areas seen at the carotid bifurcation represent calcifications (*arrowhead*). *Center*, digital subtraction angiogram showing an example of the "flame" sign (*arrow*) in a case of flow-limiting cervical ICA dissection. *Right*, digital subtraction angiogram confirming an extensive dissection of the common carotid artery with multiple intimal flaps (*arrows*)

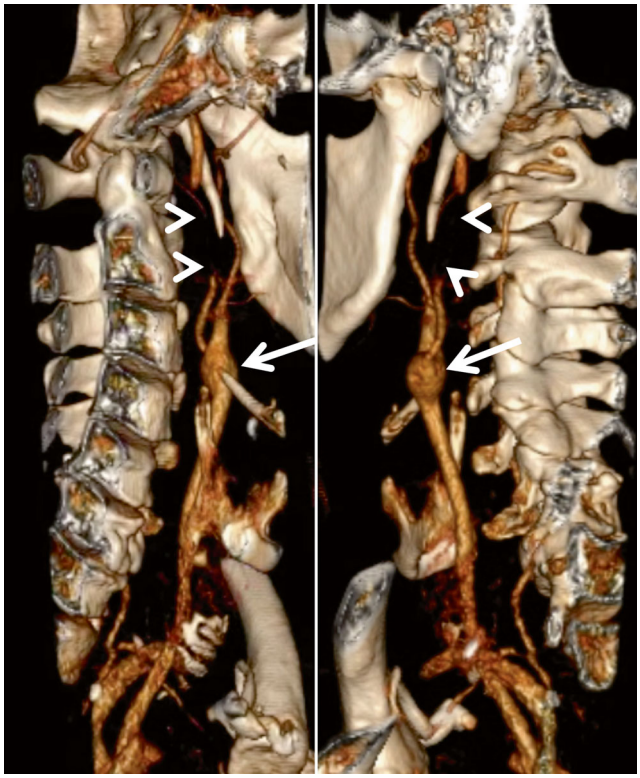

Fig. 10 A case of acute stroke with flow-limiting cervical dissection treated with carotid stenting. Volume-rendered 3D reconstruction of a neck CT angiogram demonstrated a filling defect within the proximal cervical ICA, suspicious for a flow-limiting dissection. Ipsilateral (*left*) and contralateral (*right*) views of 3D-reconstructed image are shown. *Arrows* point to the location of the carotid bulb. *Arrowheads* indicate the location of the filling defect

territory affected. Wallenberg syndrome (lateral medullary syndrome) is known for its particularly high association with

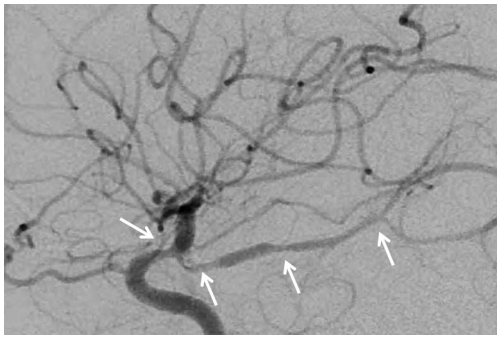

Fig. 12 Digital subtraction angiogram, ICA injection with oblique lateral view, in a patient with suspected RCVS. Multiple areas of vessel narrowing are seen (*arrows*)

vertebral artery dissection, which is reported in as many as 30–50 % of lateral medullary syndrome cases [48, 49].

Both CTA and MRA are noninvasive tests that are frequently used in clinical practice to establish the diagnosis of cervical dissection. Also, when coupled with brain MR imaging, the diffusion-weighted imaging (DWI) sequence allows excellent recognition of even subtle acute ischemic changes within the brain. MRA with a fat-suppression sequence (so-called dissection protocol) allows visualization of an intraluminal hematoma resulting from an intimal tear on the axial images. The evolution of blood products within the hematoma changes over time, and the appearance of the hematoma on the T1- and T2-weighted images can help determine the timing of when dissection occurred [50]. TOF angiography technique allows imaging without the use of gadolinium contrast. The accuracy of the TOF MRA with fat-suppressed T1 images is comparable to CE MRA for detection of cervical dissection, which can be of value in patients with renal insufficiency [51]. Depending on the surrounding structures, such

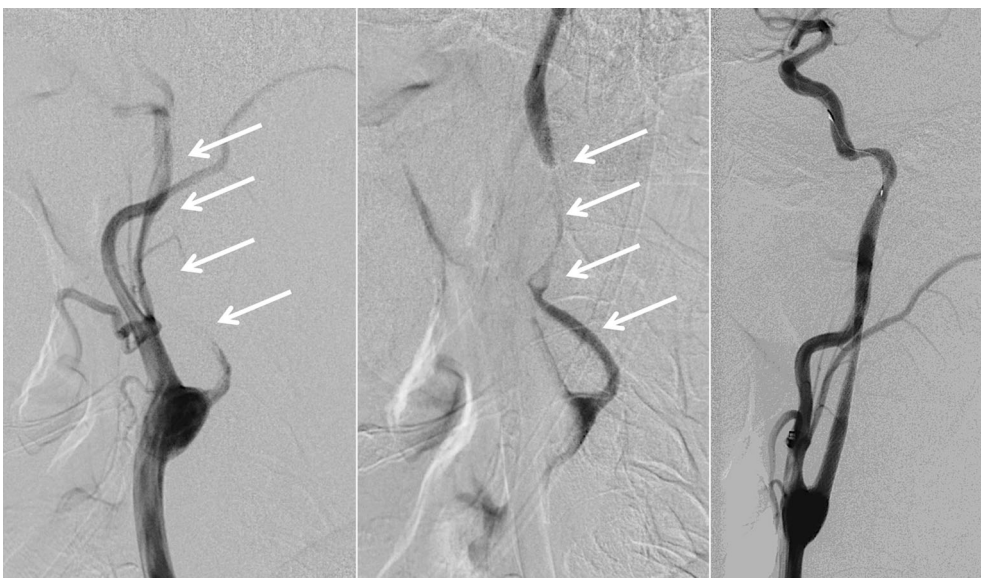

Fig. 11 Digital subtraction angiography from the case described in Fig. 10 shows a flow-limiting dissection of the cervical ICA. Notice the delay in contrast material flow beyond the dissected segment during the early (*left*) and late (*center*) phases of the angiographic run, in comparison to robust filling of the external carotid artery branches. *Arrows* point to the ICA segments with contrast stasis. *Right*, carotid stenting was performed in this case, with successful restoration of blood flow

as the amount of fat tissue, proximity to the venous plexus, or CSF, the sensitivity of MRA in detecting dissection can be affected [52].

CTA is marginally better than MRA in detecting fine anatomical features of cervical dissections, such as intimal flaps, pseudoaneurysms, and high-grade stenosis and might be favored for detection of vertebral dissections [53]. However, in many cases, both of these noninvasive approaches provide complementary information [53]. CTA is typically avoided in cases of renal insufficiency, pregnancy, or in younger patients because concerns for an accumulating radiation dose.

Although both CTA and MRA are highly accurate in detecting cervical dissection, DSA remains the gold standard and should be used for definitive diagnosis when clinically indicated, especially if endovascular treatment is being considered [54]. The benefit of DSA should be weighed against its risks given the invasive nature of this procedure. Typical radiographic findings of cervical dissection on DSA include the so-called string sign (an irregular narrow segment of the affected vessel), the "flame" sign (a tapered cutoff of the vessel), and visualization of a false lumen or an intimal flap (Figs. 9, 10, and 11). Fibromuscular dysplasia, which is frequently associated with spontaneous cervical dissection, can often be recognized by findings of multiple areas of vessel dilatation and stenosis.

Headaches Due to Reversible Cerebral Vasoconstriction Syndrome

The condition of reversible cerebral vasoconstriction syndrome (RCVS) is being increasingly recognized in the literature and can also be referred to as Call-Fleming syndrome, isolated benign cerebral vasculitis, or postpartum angiopathy [55]. RCVS frequently occurs during the postpartum period, and headaches are the most frequent symptom. Although headaches are frequently sudden and severe at onset and are often accompanied by nausea, vomiting, or photophobia, RCVS can also present with gradual insidious headache onset [56, 57]. Because headaches are a common manifestation of other conditions, such as central nervous system vasculitis, and the pattern and characteristics of headache can be nonspecific, CSF analysis and imaging data are necessary to establish the diagnosis of RCVS [55, 58, 59].

Convexity SAH can be seen in some cases of RCVS. To differentiate it from aneurysmal SAH, which carries a worse prognosis and requires a different management strategy, catheter angiography is typically performed [60, 61]. Angiography shows areas of focal segmental narrowing alternating with dilatation in RCVS, which resolves on follow-up imaging (Fig. 12) [62]. Findings on brain CT imaging and MR imaging can be quite variable and include SAH, parenchymal hematomas, and areas of ischemic infarction and edema [62–64].

Conclusion

Headaches from vascular causes need to be identified and the vascular causes need to be emergently treated to avoid dire consequences. This review summarizes the clinical presentation and imaging evaluation of different vascular causes for headache. This will serve to guide physicians in identifying patient with vascular headaches and choosing and interpreting the necessary imaging studies.

Compliance with Ethics Guidelines

Conflict of Interest Dr. Sabareesh K. Natarajan and Dr. Ashish Sonig each declares no potential conflicts of interest.

Dr. Maxim Mokin reports a grant from Toshiba.

Dr. Elad I. Levy reports other from Intratech Medical Ltd, other from Blockade Medical LLC, other from Abbott, outside the submitted work; and Principal investigator: Covidien US SWIFT PRIME Trials (for stent retrievers in acute ischemic stroke).

Human and Animal Rights and Informed Consent This article does not contain any studies with human or animal subjects performed by any of the authors.

References

Papers of particular interest, published recently, have been highlighted as:

- • Of importance
- •• Of major importance

1. Headache Classification Subcommittee of the International Headache Society. The international classification of headache disorders: 2nd edition. Cephalalgia. 2004;24 Suppl 1:9–160.
2. Dodick DW. Pearls: headache. Semin Neurol. 2010;30(1):74–81.
3. • Connolly Jr ES, Rabinstein AA, Carhuapoma JR, Derdeyn CP, Dion J, Higashida RT, et al. Guidelines for the management of aneurysmal subarachnoid hemorrhage: a guideline for healthcare professionals from the American Heart Association/American Stroke Association. Stroke. 2012;43(6):1711–37. *Good summary of current guidelines for diagnosis and management of SAH.*
4. Bederson JB, Connolly Jr ES, Batjer HH, Dacey RG, Dion JE, Diringer MN, et al. Guidelines for the management of aneurysmal subarachnoid hemorrhage: a statement for healthcare professionals from a special writing group of the Stroke Council, American Heart Association. Stroke. 2009;40(3):994–1025.
5. Linn FH, Wijdicks EF, van der Graaf Y, Weerdesteyn-van Vliet FA, Bartelds AI, van Gijn J. Prospective study of sentinel headache in aneurysmal subarachnoid haemorrhage. Lancet. 1994;344(8922):590–3.
6. Polmear A. Sentinel headaches in aneurysmal subarachnoid haemorrhage: what is the true incidence? A systematic review. Cephalalgia. 2003;23(10):935–41.
7. Edlow JA, Caplan LR. Avoiding pitfalls in the diagnosis of subarachnoid hemorrhage. N Engl J Med. 2000;342(1):29–36.
8. McCormack RF, Hutson A. Can computed tomography angiography of the brain replace lumbar puncture in the evaluation of acute-onset headache after a negative noncontrast cranial computed tomography scan? Acad Emerg Med. 2010;17(4):444–51.

9. Wang H, Li W, He H, Luo L, Chen C, Guo Y. 320-detector row CT angiography for detection and evaluation of intracranial aneurysms: comparison with conventional digital subtraction angiography. Clin Radiol. 2013;68(1):e15–20.
10. Romijn M, Gratama van Andel HA, van Walderveen MA, Sprengers ME, van Rijn JC, van Rooij WJ, et al. Diagnostic accuracy of CT angiography with matched mask bone elimination for detection of intracranial aneurysms: comparison with digital subtraction angiography and 3D rotational angiography. AJNR Am J Neuroradiol. 2008;29(1):134–9.
11. Zhang LJ, Wu SY, Niu JB, Zhang ZL, Wang HZ, Zhao YE, et al. Dual-energy CT angiography in the evaluation of intracranial aneurysms: image quality, radiation dose, and comparison with 3D rotational digital subtraction angiography. AJR Am J Roentgenol. 2010;194(1):23–30.
12. Ishihara H, Kato S, Akimura T, Suehiro E, Oku T, Suzuki M. Angiogram-negative subarachnoid hemorrhage in the era of three dimensional rotational angiography. J Clin Neurosci. 2007;14(3):252–5.
13. van Rooij WJ, Peluso JP, Sluzewski M, Beute GN. Additional value of 3D rotational angiography in angiographically negative aneurysmal subarachnoid hemorrhage: how negative is negative? AJNR Am J Neuroradiol. 2008;29(5):962–6.
14. Yuan MK, Lai PH, Chen JY, Hsu SS, Liang HL, Yeh LR, et al. Detection of subarachnoid hemorrhage at acute and subacute/chronic stages: comparison of four magnetic resonance imaging pulse sequences and computed tomography. J Chin Med Assoc. 2005;68(3):131–7.
15. Verma RK, Kottke R, Andereggen L, Weisstanner C, Zubler C, Gralla J, et al. Detecting subarachnoid hemorrhage: comparison of combined FLAIR/SWI versus CT. Eur J Radiol. 2013;82(9):1539–45.
16. Sailer AM, Wagemans BA, Nelemans PJ, de Graaf R, van Zwam WH. Diagnosing intracranial aneurysms with MR angiography: systematic review and meta-analysis. Stroke. 2014;45(1):119–26.
17. Bakker NA, Groen RJ, Foumani M, Uyttenboogaart M, Eshghi OS, Metzemaekers JD, et al. Repeat digital subtraction angiography after a negative baseline assessment in nonperimesencephalic subarachnoid hemorrhage: a pooled data meta-analysis. J Neurosurg. 2014;120(1):99–103.
18. Bruce BB, Biousse V, Newman NJ. Third nerve palsies. Semin Neurol. 2007;27(3):257–68.
19. Keane JR. Third nerve palsy: analysis of 1400 personally-examined inpatients. Can J Neurol Sci. 2010;37(5):662–70.
20. Goldenberg-Cohen N, Curry C, Miller NR, Tamargo RJ, Murphy KP. Long term visual and neurological prognosis in patients with treated and untreated cavernous sinus aneurysms. J Neurol Neurosurg Psychiatry. 2004;75(6):863–7.
21. Wiebers DO. Unruptured intracranial aneurysms: natural history and clinical management. Update on the international study of unruptured intracranial aneurysms. Neuroimaging Clin N Am. 2006;16(3):383–90. *vii*.
22. Jeong HW, Seo JH, Kim ST, Jung CK, Suh SI. Clinical practice guideline for the management of intracranial aneurysms. Neurointervention. 2014;9(2):63–71.
23. Stapf C, Mast H, Sciacca RR, Choi JH, Khaw AV, Connolly ES, et al. Predictors of hemorrhage in patients with untreated brain arteriovenous malformation. Neurology. 2006;66(9):1350–5.
24. Hernesniemi JA, Dashti R, Juvela S, Vaart K, Niemela M, Laakso A. Natural history of brain arteriovenous malformations: a long-term follow-up study of risk of hemorrhage in 238 patients. Neurosurgery. 2008;63(5):823–9. *discussion 9–31*.
25. Ondra SL, Troupp H, George ED, Schwab K. The natural history of symptomatic arteriovenous malformations of the brain: a 24-year follow-up assessment. J Neurosurg. 1990;73(3):387–91.
26. Laakso A, Hernesniemi J. Arteriovenous malformations: epidemiology and clinical presentation. Neurosurg Clin N Am. 2012;23(1):1–6.
27. Gross BA, Du R. Natural history of cerebral arteriovenous malformations: a meta-analysis. J Neurosurg. 2013;118(2):437–43.
28.•• Mokin M, Dumont TM, Levy EI. Novel multimodality imaging techniques for diagnosis and evaluation of arteriovenous malformations. Neurol Clin. 2014;32(1):225–36. *Good review of imaging techniques that help in the diagnosis and management of AVMs*.
29. Strother CM, Bender F, Deuerling-Zheng Y, Royalty K, Pulfer KA, Baumgart J, et al. Parametric color coding of digital subtraction angiography. AJNR Am J Neuroradiol. 2010;31(5):919–24.
30. Gandhi D, Chen J, Pearl M, Huang J, Gemmete JJ, Kathuria S. Intracranial dural arteriovenous fistulas: classification, imaging findings, and treatment. AJNR Am J Neuroradiol. 2012;33(6):1007–13.
31. van Dijk JM, terBrugge KG, Willinsky RA, Wallace MC. Clinical course of cranial dural arteriovenous fistulas with long-term persistent cortical venous reflux. Stroke. 2002;33(5):1233–6.
32. Natarajan SK, Ghodke B, Kim LJ, Hallam DK, Britz GW, Sekhar LN. Multimodality treatment of intracranial dural arteriovenous fistulas in the Onyx era: a single center experience. World Neurosurg. 2010;73(4):365–79.
33. Miller NR. Dural carotid-cavernous fistulas: epidemiology, clinical presentation, and management. Neurosurg Clin N Am. 2012;23(1):179–92.
34. Campbell PG, Jabbour P, Yadla S, Awad IA. Emerging clinical imaging techniques for cerebral cavernous malformations: a systematic review. Neurosurg Focus. 2010;29(3):E6.
35. Zabramski JM, Wascher TM, Spetzler RF, Johnson B, Golfinos J, Drayer BP, et al. The natural history of familial cavernous malformations: results of an ongoing study. J Neurosurg. 1994;80(3):422–32.
36. Steiger HJ, Markwalder TM, Reulen HJ. Clinicopathological relations of cerebral cavernous angiomas: observations in eleven cases. Neurosurgery. 1987;21(6):879–84.
37. Bousser MG, Ferro JM. Cerebral venous thrombosis: an update. Lancet Neurol. 2007;6(2):162–70.
38. Wasay M, Kojan S, Dai AI, Bobustuc G, Sheikh Z. Headache in cerebral venous thrombosis: incidence, pattern and location in 200 consecutive patients. J Headache Pain. 2010;11(2):137–9.
39. Crassard I, Bousser MG. Headache in patients with cerebral venous thrombosis. Rev Neurol (Paris). 2005;161(6–7):706–8.
40.•• Bonneville F. Imaging of cerebral venous thrombosis. Diagn Interv Imaging. 2014;95:1145–50. *Good review of imaging techniques for CVT*.
41. Meckel S, Reisinger C, Bremerich J, Damm D, Wolbers M, Engelter S, et al. Cerebral venous thrombosis: diagnostic accuracy of combined, dynamic and static, contrast-enhanced 4D MR venography. AJNR Am J Neuroradiol. 2010;31(3):527–35.
42. Lee VH, Brown Jr RD, Mandrekar JN, Mokri B. Incidence and outcome of cervical artery dissection: a population-based study. Neurology. 2006;67(10):1809–12.
43. Schievink WI, Roiter V. Epidemiology of cervical artery dissection. Front Neurol Neurosci. 2005;20:12–5.
44. Biller J, Sacco RL, Albuquerque FC, Demaerschalk BM, Fayad P, Long PH, et al. Cervical arterial dissections and association with cervical manipulative therapy: a statement for healthcare professionals from the American Heart Association/American Stroke Association. Stroke. 2014;45(10):3155–74.
45. Lyrer PA, Brandt T, Metso TM, Metso AJ, Kloss M, Debette S, et al. Clinical import of Horner syndrome in internal carotid and vertebral artery dissection. Neurology. 2014;82(18):1653–9.

46. Debette S, Grond-Ginsbach C, Bodenant M, Kloss M, Engelter S, Metso T, et al. Differential features of carotid and vertebral artery dissections: the CADISP study. Neurology. 2011;77(12):1174–81.
47. Dziewas R, Konrad C, Drager B, Evers S, Besselmann M, Ludemann P, et al. Cervical artery dissection—clinical features, risk factors, therapy and outcome in 126 patients. J Neurol. 2003;250(10):1179–84.
48. Hosoya T, Nagahata M, Yamaguchi K. Prevalence of vertebral artery dissection in Wallenberg syndrome: neuroradiological analysis of 93 patients in the Tohoku District, Japan. Radiat Med. 1996;14(5):241–6.
49. Fukuoka T, Takeda H, Dembo T, Nagoya H, Kato Y, Deguchi I, et al. Clinical review of 37 patients with medullary infarction. J Stroke Cerebrovasc Dis. 2012;21(7):594–9.
50. Paciaroni M, Caso V, Agnelli G. Magnetic resonance imaging, magnetic resonance and catheter angiography for diagnosis of cervical artery dissection. Front Neurol Neurosci. 2005;20:102–18.
51. Coppenrath EM, Lummel N, Linn J, Lenz O, Habs M, Nikolaou K, et al. Time-of-flight angiography: a viable alternative to contrast-enhanced MR angiography and fat-suppressed T1w images for the diagnosis of cervical artery dissection? Eur Radiol. 2013;23(10):2784–92.
52. Felber S, Auer A, Schmidauer C, Waldenberger P, Aichner F. Magnetic resonance angiography and magnetic resonance tomography in dissection of the vertebral artery. Radiologe. 1996;36(11):872–83.
53. Vertinsky AT, Schwartz NE, Fischbein NJ, Rosenberg J, Albers GW, Zaharchuk G. Comparison of multidetector CT angiography and MR imaging of cervical artery dissection. AJNR Am J Neuroradiol. 2008;29(9):1753–60.
54. Latchaw RE, Alberts MJ, Lev MH, Connors JJ, Harbaugh RE, Higashida RT, et al. Recommendations for imaging of acute ischemic stroke: a scientific statement from the American Heart Association. Stroke. 2009;40(11):3646–78.
55. Ducros A. Reversible cerebral vasoconstriction syndrome. Lancet Neurol. 2012;11(10):906–17.
56. Sattar A, Manousakis G, Jensen MB. Systematic review of reversible cerebral vasoconstriction syndrome. Expert Rev Cardiovasc Ther. 2010;8(10):1417–21.
57. Gerretsen P, Kern RZ. Reversible cerebral vasoconstriction syndrome: a thunderclap headache-associated condition. Curr Neurol Neurosci Rep. 2009;9(2):108–14.
58. Pizzanelli C, Catarsi E, Pelliccia V, Cosottini M, Pesaresi I, Puglioli M, et al. Primary angiitis of the central nervous system: report of eight cases from a single Italian center. J Neurol Sci. 2011;307(1–2):69–73.
59. Birnbaum J, Hellmann DB. Primary angiitis of the central nervous system. Arch Neurol. 2009;66(6):704–9.
60. Muehlschlegel S, Kursun O, Topcuoglu MA, Fok J, Singhal AB. Differentiating reversible cerebral vasoconstriction syndrome with subarachnoid hemorrhage from other causes of subarachnoid hemorrhage. JAMA Neurol. 2013;70(10):1254–60.
61. Mathon B, Ducros A, Bresson D, Herbrecht A, Mirone G, Houdart E, et al. Subarachnoid and intra-cerebral hemorrhage in young adults: rare and underdiagnosed. Rev Neurol (Paris). 2014;170(2):110–8.
62. Ansari SA, Rath TJ, Gandhi D. Reversible cerebral vasoconstriction syndromes presenting with subarachnoid hemorrhage: a case series. J Neurointerv Surg. 2011;3(3):272–8.
63. Marder CP, Donohue MM, Weinstein JR, Fink KR. Multimodal imaging of reversible cerebral vasoconstriction syndrome: a series of 6 cases. AJNR Am J Neuroradiol. 2012;33(7):1403–10.
64. Ducros A, Boukobza M, Porcher R, Sarov M, Valade D, Bousser MG. The clinical and radiological spectrum of reversible cerebral vasoconstriction syndrome. A prospective series of 67 patients. Brain. 2007;130(Pt 12):3091–101.